Check for
updates

Recent Advances in Planar Optics-Based Glasses-Free 3D Displays

Jianyu Hua[1,2], Wen Qiao[1,2]* and Linsen Chen[1,2,3]*

[1]School of Optoelectronic Science and Engineering, Collaborative Innovation Center of Suzhou Nano Science and Technology, Soochow University, Suzhou, China, [2]Key Lab of Advanced Optical Manufacturing Technologies of Jiangsu Province and Key Lab of Modern Optical Technologies of Education Ministry of China, Soochow University, Suzhou, China, [3]SVG Optronics, Co., Ltd, Suzhou, China
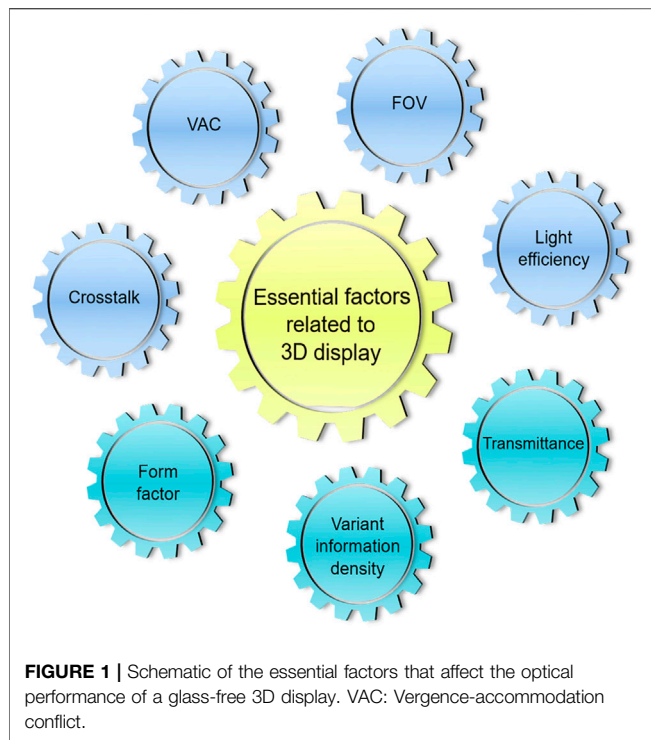
Glasses-free three-dimensional (3D) displays are one of the technologies that will redefine human-computer interfaces. However, many geometric optics-based 3D displays suffer from a limited field of view (FOV), severe resolution degradation, and visual fatigue. Recently, planar optical elements (e.g., diffraction gratings, diffractive lenses and metasurfaces) have shown superior light manipulating capability in terms of light intensity, phase, and polarization. As a result, planar optics hold great promise to tackle the critical challenges for glasses-free 3D displays, especially for portable electronics and transparent display applications. In this review, the limitations of geometric optics-based glasses-free 3D displays are analyzed. The promising solutions offered by planar optics for glasses-free 3D displays are introduced in detail. As a specific application and an appealing feature, augmented reality (AR) 3D displays enabled by planar optics are comprehensively discussed. Fabrication technologies are important challenges that hinder the development of 3D displays. Therefore, multiple micro/nanofabrication methods used in 3D displays are highlighted. Finally, the current status, future direction and potential applications for glasses-free 3D displays and glasses-free AR 3D displays are summarized.

Keywords: glasses-free 3D display, diffraction grating, metagrating, metasurface, AR 3D display, diffractive lens, holographic optical element

INTRODUCTION

Since Charles Wheatstone first invented stereoscopy, the research interest in three-dimensional (3D) displays has extended for 150 years, and its history is as long as that of photography (Charles, 1838). As a more natural way to present virtual data, glasses-free 3D displays show great prospects in various fields including education, military, medical, entertainment, automobile, etc. According to a survey, people spend an average of 5 h every day watching display panel screens. The visualization of 3D images will have a huge impact on improving work efficiency. Therefore, glasses-free 3D displays are regarded as next-generation display technology.

Generally, we assign glasses-free 3D displays into three main categories: holographic 3D displays, volumetric 3D displays and autostereoscopic 3D displays (Geng, 2013). A holographic 3D display is a technology that records both the amplitude and phase information of a real object and reproduces it through specific mediums (e.g., photorefractive polymers) (Tay et al., 2008; Blanche et al., 2010). Furthermore, by using a spatial light modulator that directly modulates the coherent wave,

FIGURE 1 | Schematic of the essential factors that affect the optical performance of a glass-free 3D display. VAC: Vergence-accommodation conflict.
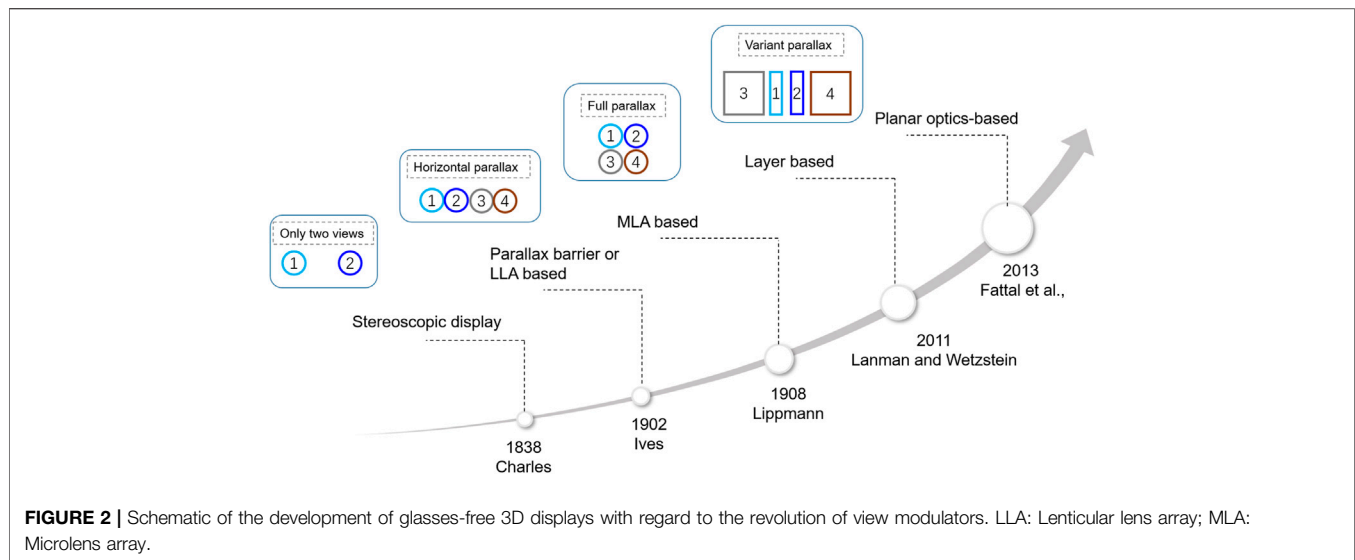
computer-generated hologram systems can be implemented via numerical simulation. (Hahn et al., 2008; Sasaki et al., 2014). Currently, powerful acceleration chips or video processors have enabled the reproduction of high-quality 3D holograms at video rates (An et al., 2020; Shi et al., 2021). In the future, real-time holographic 3D displays will have wide applications in mobile displays and AR displays (Peng et al., 2021; Lee et al., 2022). Volumetric 3D display is another technology that generates luminous image points (i.e., voxels) in space via special media, such as trapped particles and fluorescent screens. These image points form 3D graphics that can be observed within 360° (Kumagai et al., 2015; Kumagai et al., 2018; Smalley et al., 2018; Hirayama et al., 2019). Both the holographic 3D display and volumetric 3D display require a large amount of data to provide 3D content, which brings challenges to data processing and transportation.

In contrast, autostereoscopic 3D displays reduce computing costs by discretizing a continuously distributed light field of 3D objects into multiple "views". The properly arranged perspective views can approximate the 3D images with motion parallax and stereo parallax. Moreover, by modulating the irradiance pattern of each view, only a small number of views are required to reconstruct the light field. A typical autostereoscopic 3D display only needs to integrate two components: an optical element and an off-the-shelf refreshable display panel (e.g., liquid crystal display, organic light-emitting diode display, light-emitting diode display) (Dodgson, 2005). With the advantages of a compact form factor, ease of integration with flat display devices, ease of modulation, and low cost, autostereoscopic

3D displays can be applied in portable electronics and redefine human-computer interfaces. The function of the optical element in an autostereoscopic 3D display is to manipulate the incident light and generate a finite number of views. To improve the display effect, the optical elements also need to modulate the views and angular separation between views, which is called the "view modulator" in this paper. View modulators represent a special class of optical elements that are used in glass-free 3D displays for view modulation, such as parallax barriers, lenticular lens arrays, and metagratings.

One of the most critical issues in autostereoscopic 3D displays is how to design view modulators. When we design view modulators, several essential problems need to be considered that are directly related to 3D display performance (**Figure 1**): 1) To minimize crosstalk and ghost images, the view modulators should confine the emerging light within a well-defined region; 2) To address the vergence-accommodation conflict, the view modulators need to provide both correct vergence and accommodation cues. Vergence-accommodation conflict occurs when the depth of 3D images induced by binocular parallax lies in front of or behind the display screen, whereas the depth recognized by a single eye is fixed at the apparent location of the physical display panel because the image observed by a single eye is 2D (Zou et al., 2015; Koulieris et al., 2017); 3) To achieve a large field of view (FOV), the view modulators need to precisely manipulate light over a large steering angle; 4) For an energy-efficient system, the light efficiency of the view modulators needs to be adequate. In addition to these four important factors that affect the optical performance of 3D displays, there are some additional features that should be addressed in applications; 5) To maintain a thin form factor and be lightweight for portable electronics, the design of view modulators should be elegant with as few layers or components as possible; 6) To solve the tradeoff between spatial resolution, angular resolution, and FOV, the view modulators should manipulate the shape of view for variant information density. 7) In window display applications, the view modulators should be transparent to combine virtual 3D images with physical objects for glasses-free augmented reality display.

Depending on the types of adopted view modulators, autostereoscopic 3D displays can be divided into geometrical optics-based and planar optics-based systems. With regard to geometrical optics-based 3D displays, the most representative architectures are parallax barrier or lenticular lens array-based, microlens array-based and layer-based systems (Ma et al., 2019). The parallax barrier or lenticular lens array was first integrated with flat panels and applied in 3D mobile electronic devices because of the advantages of utilizing existing 2D screen fabrication infrastructure (Ives, 1902; Kim et al., 2016; Yoon et al., 2016; Lv et al., 2017; Huang et al., 2019). For improved display performance, aperture stops were inserted into the system to reduce the crosstalk by decreasing the aperture ratio; however, this strategy comes at the expense of light efficiency (Wang et al., 2010; Liang et al., 2014; Lv et al., 2014). Microlens array-based 3D

FIGURE 2 | Schematic of the development of glasses-free 3D displays with regard to the revolution of view modulators. LLA: Lenticular lens array; MLA: Microlens array.
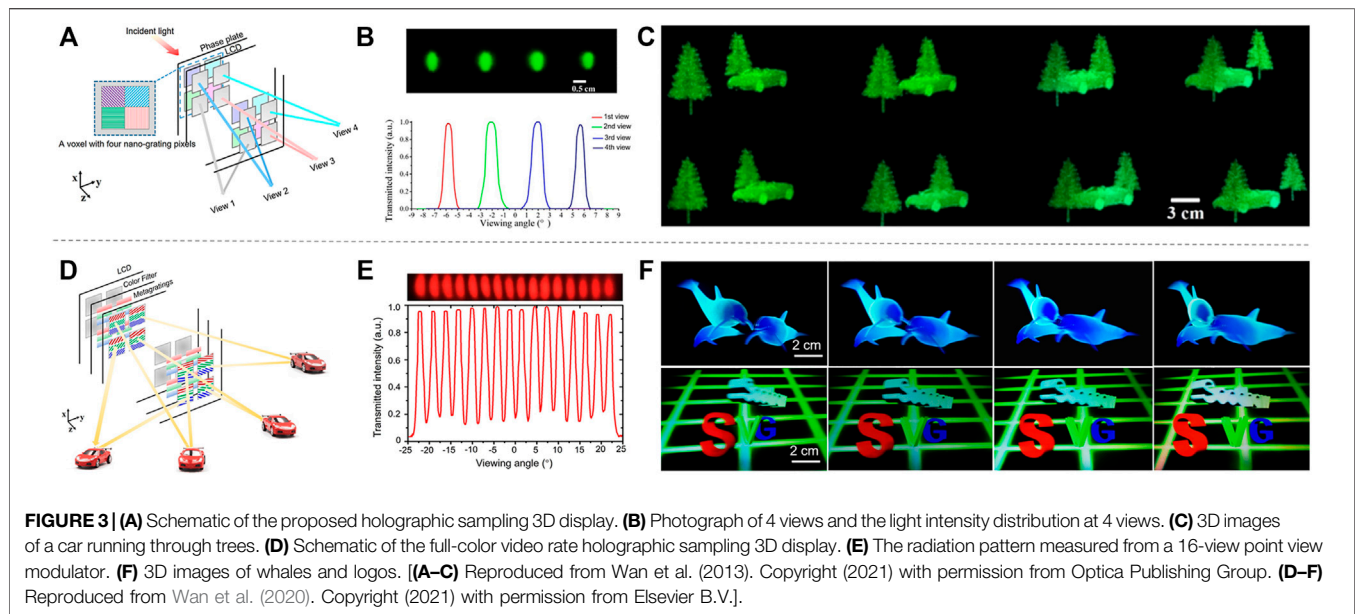
display, i.e., integral imaging display generates stereoscopic images by recording and reproducing the rays from 3D objects (Lippmann, 1908; Martínez-Corral and Javidi, 2018; Javidi et al., 2020). It can present full motion parallax by adding light manipulating power in a different direction. Recently, a bionic compound eye structure was proposed to enhance the performance of integral imaging 3D display systems. With proper design based on geometric optics, the 3D display prototype can be used to obtain a 28° horizontal, 22° vertical viewing angle, approximately two times that of a normal integral imaging display (Zhao et al., 2020). In another work, an integral imaging 3D display system that can enhance both the pixel density and viewing angle was proposed, with parallel projection of ultrahigh-definition elemental images (Watanabe et al., 2020). This prototype display system reproduced 3D images with a horizontal pixel density of 63.5 ppi and viewing angles of 32.8° and 26.5° in the horizontal and vertical directions, respectively. Furthermore, with three groups of directional backlight and a fast-switching liquid crystal display (LCD) panel, a time-multiplexed integral imaging 3D display with a 120° wide viewing angle was demonstrated (Liu et al., 2019). The layer-based 3D display invented by Lanman and Wetzstein (Lanman et al., 2010; Lanman et al., 2011; Wetzstein et al., 2011; Wetzstein et al., 2012) used multiple LCD screen layers to modulate the light field of 3D objects. This display can provide both vergence and accommodation cues for viewers with limited fatigue and dizziness (Maimone et al., 2013). Nevertheless, its FOV is limited by the effective size of the display panel. Moreover, layer-based 3D displays also suffer from a trade-off between the depth of field and the complexity of the system (i.e., the layer number for the display devices). In general, geometrical optics-based autostereoscopic 3D displays have the advantages of low cost and thin form factors that are compatible with 2D flat display panels. However, we still have a fair way to go due to the tradeoffs among the resolution, FOV, depth cues, depth of field and form factor (Qiao et al., 2020). Alleviating these tradeoffs and improving the image quality to provide more realistic

stereoscopic vision has opened up an intriguing avenue for developing next-generation 3D display technology.

Fast-growing planar optics have attracted wide attention in various fields because of their outstanding capability for light control (Genevet et al., 2017; Zhang and Fang, 2019; Chen and Segev, 2021; Tabiryan et al., 2021; Xiong and Wu, 2021). In the field of glasses-free 3D displays, planar optical elements, such as diffraction gratings, diffractive lenses and metasurfaces, can be used to modulate the light field of 3D objects at the pixel level. With proper design, planar optical elements at the micro or nano scale provide superior light manipulation capability in terms of light intensity, phase, and polarization. Therefore, planar optics-based glass-free 3D displays have several merits, such as reduced crosstalk, no vergence-accommodation conflict, enhanced light efficiency, and an enlarged FOV. **Figure 2** shows the developing trend for 3D display technologies with regard to the revolution of view modulators. Planar optics are becoming the "next-generation 3D display technology" because of outstanding view modulation flexibility.

In this review, the critical challenges for glasses-free 3D displays are analyzed. Planar optics-based 3D displays suggest a variety of solutions for 3D displays, which will be reviewed in the section *Glasses-Free 3D Display Based on Planar Optical Elements*. As a specific application and an appealing feature, augmented reality (AR) 3D displays enabled by planar optics will be comprehensively introduced in the section *Glasses-Free augmented reality 3D display based on planar optical elements*. In addition to the design of view modulators, the fabrication of view modulators is another challenge that hinders the development of 3D displays. Therefore, in the section *Fabrication of Large-Scale Micro/Nanostructures on View Modulators for 3D Displays*, we will highlight multiple micro/nanofabrication methods for view modulators in 3D displays. In the section *Conclusions and Outlook*, the current status for glasses-free 3D displays and glasses-free AR 3D displays will be summarized. Finally, future directions and potential applications are suggested in the section *Conclusions and Outlook*.

FIGURE 3 | (A) Schematic of the proposed holographic sampling 3D display. **(B)** Photograph of 4 views and the light intensity distribution at 4 views. **(C)** 3D images of a car running through trees. **(D)** Schematic of the full-color video rate holographic sampling 3D display. **(E)** The radiation pattern measured from a 16-view point view modulator. **(F)** 3D images of whales and logos. [**(A–C)** Reproduced from Wan et al. (2013). Copyright (2021) with permission from Optica Publishing Group. **(D–F)** Reproduced from Wan et al. (2020). Copyright (2021) with permission from Elsevier B.V.].

GLASSES-FREE AUGMENTED REALITY 3D DISPLAY BASED ON PLANAR OPTICAL ELEMENTS

3D Display Based on Diffraction Gratings

Diffraction gratings are unique components that can split incident light into many spatial directions simultaneously and have been widely used in steering devices, such as spectrometers, optical waveguides and laser resonators (Zola et al., 2019; Cao et al., 2020; Görrn et al., 2011; Zhang et al., 2019; Liu et al., 2020). Fattal et al. employed diffraction gratings in a 3D display and proposed a directional diffractive backlight to produce full parallax views within a wide FOV (Fattal et al., 2013). The key elements in the backlight were pixelated grating patterns fabricated by electron-beam lithography. Both passive and active prototypes provided 64-view images within a FOV of 90°. The diffractive wide-angle backlight is regarded as a revolutionary 3D display (https://www.technologyreview.com/innovator/david-fattal). It has opened up rich opportunities for planar optics-based glasses-free 3D displays.
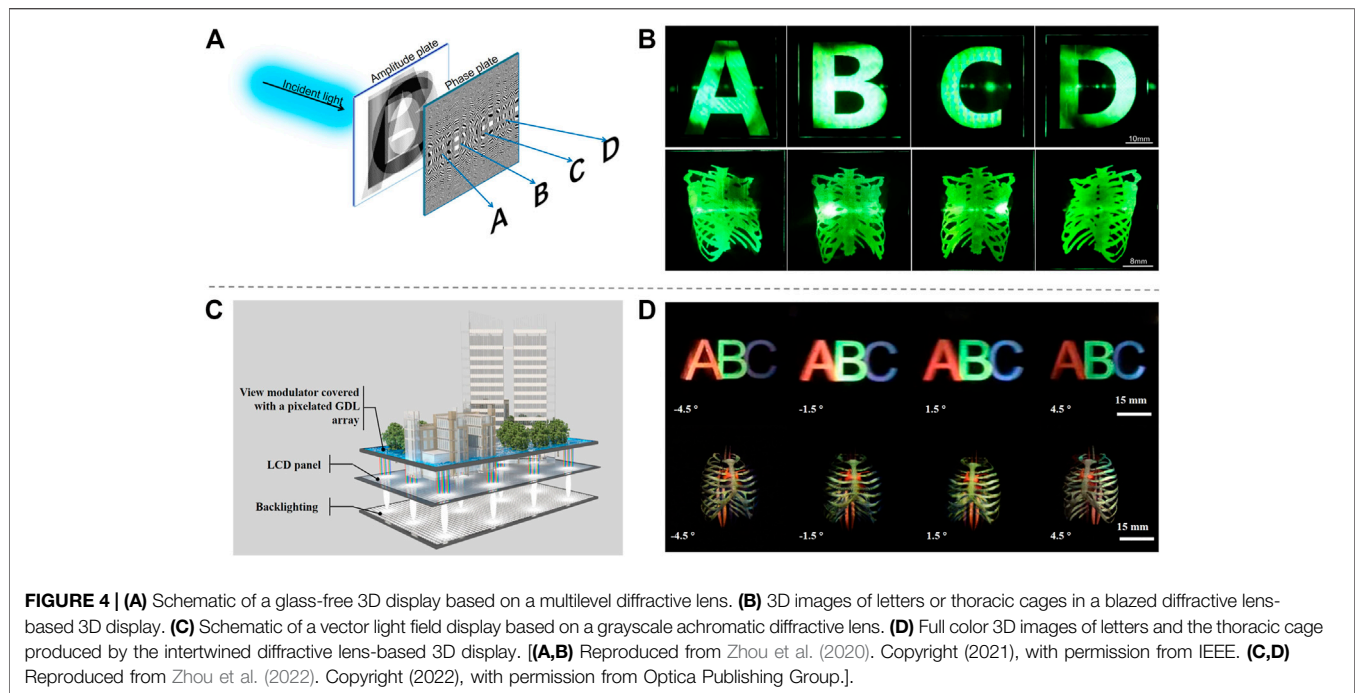
On this basis, a holographic sampling 3D display was proposed by combining a phase plate with a thin film transistor-LCD panel (Wan et al., 2017) (**Figure 3A**). The phase plate modulates the phase information, while the LCD panel provides refreshable amplitude information for the light field. Notably, the period and orientation of the diffraction gratings in each pixel are calculated to form converged beams instead of (semi)parallel beams in a geometrical optics-based 3D display. As a result, the angular divergence of target viewpoints (1.02°) is confined close to the diffraction limit (0.94°), leading to significantly reduced crosstalk and ghost images (**Figures 3B,C**). The researchers further presented a holographic sampling 3D display based on metagratings and demonstrated a video rate full-color 3D display prototype with sizes ranging from 5 to 32 inches

(**Figure 3D**) (Wan et al., 2020). The metagratings on the view modulator were designed to operate at the R/G/B wavelength to reconstruct the wavefront at sampling viewpoints with the correct white balance (**Figure 3E**). By combining the view modulator, a LCD panel and a color filter, virtual 3D whales were presented, as shown in **Figure 3F**. To address the vergence-accommodation conflict in 3D displays, a super multiview display was also proposed based on pixelated gratings. Closely packaged views with an angular separation of 0.9° provide a depth cue for the accommodation process of the human eye (Wan et al., 2020).

To summarize, diffraction grating-based 3D displays have the advantages of minimum crosstalk, reduced vergence-accommodation conflict, tailorable view arrangement, continuous motion parallax and a wide FOV. Nevertheless, the experimental diffraction efficiency of binary gratings is approximately 20%, leading to inevitable high-power consumption. On this basis, diffractive lenses and metasurfaces are employed for 3D displays.

3D Display Based on a Diffractive Lens

Recently, there has been wide interest in diffractive lenses (Huang et al., 2018; Banerji et al., 2019). The focusing effect of a diffractive lens can be equal to or even surpass that of a geometric lens. To increase the light efficiency, a blazed or multilevel diffraction lens was proposed with an approximately continuous phase delay (Fleming and Hutley, 1997). To reduce the dispersion caused by diffraction for broadband wavelength imaging, a harmonic lens was proposed based on multiple orders of diffraction (Faklis and Morris, 1995; Sweeney and Sommargren, 1995). Furthermore, continuous broadband diffractive optics were also developed for the visible (Wang et al., 2016; Mohammad et al., 2017; Meem et al., 2018; Mohammad et al., 2018), longwave infrared (Meem et al., 2019) and terahertz spectral bands (Banerji and Sensale-Rodriguez, 2019). To enhance the depth of field, a multilevel diffraction lens was proposed that can be used to focus beams

FIGURE 4 | (A) Schematic of a glass-free 3D display based on a multilevel diffractive lens. **(B)** 3D images of letters or thoracic cages in a blazed diffractive lens-based 3D display. **(C)** Schematic of a vector light field display based on a grayscale achromatic diffractive lens. **(D)** Full color 3D images of letters and the thoracic cage produced by the intertwined diffractive lens-based 3D display. [**(A,B)** Reproduced from Zhou et al. (2020). Copyright (2021), with permission from IEEE. **(C,D)** Reproduced from Zhou et al. (2022). Copyright (2022), with permission from Optica Publishing Group.].

from 5 to 1,200 mm (Banerji et al., 2020). Furthermore, with feature sizes in the range of several to several hundred microns, diffractive lenses are accessible for low-cost, large-area volume manufacturing.

Light efficiency is a crucial parameter in glass-free 3D display systems. Diffractive lenses with blazed structures can be used to focus light together, thereby showing higher light efficiency in 3D displays than diffraction gratings. As shown in **Figures 4A,B**, pixelated blazed diffractive lenses are introduced in a 3D display to form four independent convergent views, while the amplitude plate provides the images at these views. The system has the following benefits. First, each structured pixel on the view modulator is calculated by the relative position relationship between the pixel and viewing points. These accurately calculated aperiodic structures can improve the precision of light manipulation, thereby eliminating crosstalk and ghost images. Second, the 4-level blazed diffractive lens greatly increases the diffraction efficiency of the grating-based 3D display from 20 to 60% (Zhou et al., 2020). In another work, a view modulator covered with a blazed diffractive lenticular lens was proposed in a multiview holographic 3D display (Hua et al., 2020). This system redirected the diverging rays to shape four extended views with a vertical FOV of 17.8°. In addition, the diffraction efficiency of the view modulator was increased to 46.9% using the blazed phase structures. Most recently, a vector light field display with a large depth of focus was proposed based on an intertwined flat lens, as shown in **Figures 4C,D**. A grayscale achromatic diffractive lens was designed to extend the depth of focus by 1.8×10^4 times. By integrating the intertwined diffractive lens with a liquid crystal display, a 3D display with a crosstalk below 26% was realized over a viewing distance ranging from 24 to 90 cm (Zhou et al., 2022).

In summary, coupled with various design approaches, an optimized diffractive lens can enable the realization of a high-quality full spectrum in imaging applications (Peng et al., 2015; Heide et al., 2016; Peng et al., 2016; Peng et al., 2019). The design of diffractive lenses in 3D displays bears similarities to the design in imaging. This solves the problem of light efficiency in diffractive grating-based 3D displays. The optimized lens features a high light efficiency, wide spectrum response and large depth of focus, which benefits glasses-free 3D displays in terms of brightness, color fidelity, and viewing depth. However, the minimum feature size of diffractive lenses is generally larger than that of nanogratings due to the fabrication limit, resulting in a reduced viewing angle.

3D Display Based on Metasurfaces

Metamaterials are artificially engineered materials built from assemblies of nanostructures. The possessed properties, such as negative refraction (Shelby et al., 2001; Valentine et al., 2008), perfect absorption (Qian et al., 2017; Zhou et al., 2021), and invisibility cloaking (Ergin et al., 2010), are not found in naturally occurring materials (Jiang et al., 2019). As a special class of metamaterials, metasurfaces can generate controllable abrupt interfacial phase changes using a single-layer metal or dielectric nanostructures to realize wavefront regulation at the subwavelength scale. A plethora of applications have already been demonstrated in various optical elements, such as metalenses (Khorasaninejad et al., 2016; Chen et al., 2018; Wang et al., 2021), holograms (Zheng et al., 2015; Huang et al., 2018; Intaravanne et al., 2021), spectrometers (Zhu et al., 2017; Faraji-Dana et al., 2018), and vortex beam generators (Yue et al., 2016; Zhang et al., 2018). Compared with traditional optical elements and diffractive optical
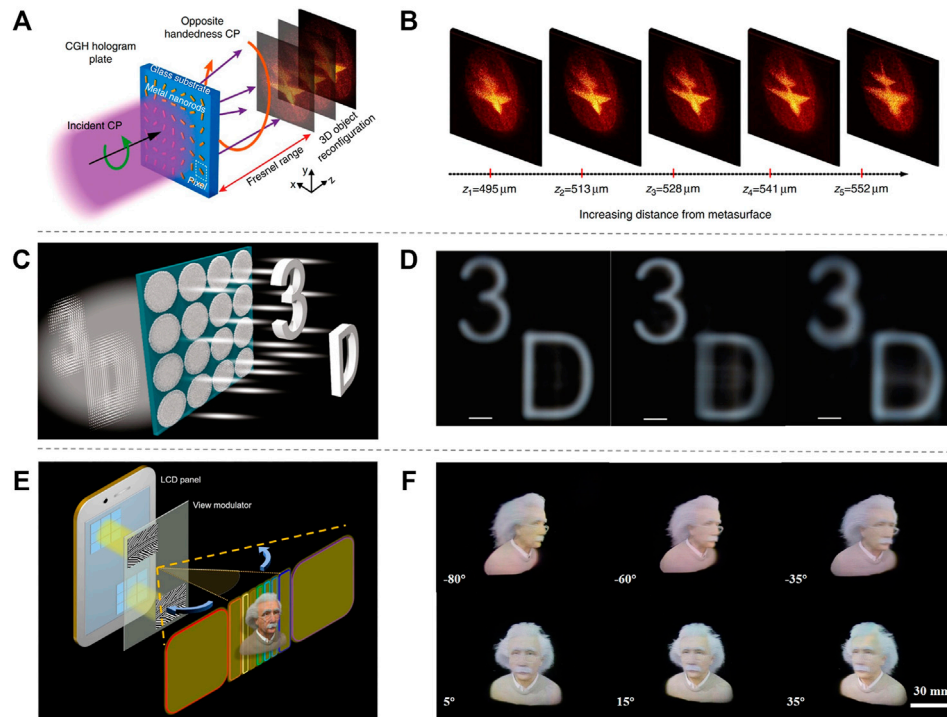
FIGURE 5 | (A) Schematic of a plasmonic metasurface for 3D CGH image reconstruction. **(B)** Experimental hologram images for different focusing positions along the z direction. **(C)** Schematic of the broadband achromatic metalens array for a white-light achromatic integral imaging display. **(D)** Reconstructed images for the cases that "3" and "D" lie on the same depth plane or on different depth planes, respectively. Scale bar, 100 µm. **(E)** Schematic of a foveated glasses-free 3D display using the two-dimensional metagrating complex. **(F)** "Albert Einstein" images in the foveated 3D display system. [**(A,B)** Reproduced from Huang et al. (2013). Copyright (2021), with permission from Springer Nature. **(C,D)** Reproduced from Fan et al. (2019). Copyright (2021), with permission from Springer Nature. **(E,F)** Reproduced from Hua et al. (2021). Copyright (2021), with permission from Springer Nature.].

elements, metasurfaces have the advantages of broadband light manipulation, flexible design and pixels at a subwavelength size.

We believe that metasurfaces can be used in 3D displays because of their unprecedented capability to manipulate light fields. In 2013, 3D computer-generated holography image reconstruction was demonstrated in the visible and near-infrared range by a plasmonic metasurface composed of pixelated gold nanorods (Huang et al., 2013) (**Figures 5A,B**). The pixel size of the metasurface hologram was only 500 nm, which is much smaller than the size of the hologram pixels generated by spatial light modulators or diffractive optical elements. As a result, a FOV as large as 40° was demonstrated. To correct chromatic aberration in integral imaging 3D displays, a single polarization-insensitive broadband achromatic metalens using silicon nitride was proposed (Fan et al., 2019) (**Figures 5C,D**). Each achromatic metalens has a diameter of 14 µm and was fabricated via the electron beam lithography technique. The focusing efficiency was 47% on average. By composing a 60×60 metalens in a rectangular lattice, a broadband achromatic integral imaging display was demonstrated under white light illumination. To address the tradeoff between spatial resolution, angular resolution, and FOV, a general approach for foveated glasses-free 3D displays using the two-dimensional metagrating complex was proposed recently (**Figure 5E**) (Hua et al., 2021). The dot/linear/rectangular

hybrid views, which are shaped by a two-dimensional metagrating complex, form spatially variant information density. By combining the two-dimensional metagrating complex film and a LCD panel, a video rate full-color foveated 3D display system with an unprecedented FOV up to 160° was demonstrated (**Figure 5F**). Compared with prior work, the proposed system makes two breakthroughs: First, the irradiance pattern of each view can be tailored carefully to avoid both crosstalk and discontinuity between views. Second, the tradeoffs between the angular resolution, spatial resolution and FOV in 3D displays are alleviated.

To summarize, metasurfaces provide a solution that maintains both a large FOV and reasonable light efficiency. Moreover, the superior light manipulation capability provides an inspiring foveated glasses-free 3D display solution for an intrinsic tradeoff between resolution and viewing angle in 3D displays. Like all metamaterial-based photonic devices, the mass fabrication of metasurfaces is the major issue that prevents industrial application of this technology.

A Comparison of Planar Optics-Based 3D Displays

As mentioned above, we have reviewed the research progress for planar optics-based glass-free 3D displays: diffraction grating-

TABLE 1 | A comparison of the various methods used to realize glasses-free 3D displays.

Types	Light efficiency	FOV with continuous parallax	Fabrication scaling	Viewing distance	Crosstalk	View arrangement	References
Parallax barrier based	Low	Small	Large	Limited	High	Horizontal parallax	Kim et al. (2016); Yoon et al. (2016)
Lenticular lens based	High	Small	Large	Limited	High	Horizontal parallax	Lv et al. (2017); Huang et al. (2019)
Microlens array based	High	Small	Large	Limited	High	Full parallax	Zhao et al. (2020); Watanabe et al. (2020)
Multilayer LCD based	Low	Small	Large	Limited	High	Full parallax	Lanman et al. (2010); Wetzstein et al. (2011)
Diffraction grating based	Low	Large	Large	Large	Low	Full parallax	Fattal et al. (2013); Wan et al. (2020)
Diffractive lens based	High	Small	Large	Large	Low	Full parallax	Zhou et al. (2020); Zhou et al. (2022)
Metasurfaces based	Medium	Large	Small	Large	Low	Variant view	Fan et al. (2019); Hua et al. (2021)

based, diffractive lens-based and metasurface-based. Compared with geometric optics-based 3D displays, these displays all have common advantages, such as high precision control at the pixel level, high degrees of freedom in design, and compact form factors. On the other hand, they have their own properties in terms of light efficiency, FOV, viewing distance, and fabrication scaling, as listed in **Table 1**. The diffraction grating-based method has both a large FOV with continuous motion parallax and large fabrication scaling. Although the bandwidth of the diffraction grating is limited, a full-color display can still be realized by integrating a color filter. As a result, the problem of selective bandwidth operation is trivial in 3D displays. However, the low light efficiency of binary gratings can be problematic because of the increased power consumption, especially in portable electronics. The diffractive lens-based approach greatly improves the light efficiency. Moreover, through proper design, an intertwined diffractive lens can be used to realize a large viewing distance and broadband spectrum manipulation. Nevertheless, the viewing angle of a diffractive lens-based 3D display is limited by the numerical aperture. The metasurface-based technique has the advantages of medium light efficiency, a large FOV and broadband spectrum response. Therefore, metasurfaces can provide better 3D display performance in terms of color fidelity. Furthermore, the subwavelength dimensions of metasurfaces ensure their flexibility for view manipulation. However, the complexity and difficulty in nanofabrication hinders the application of metasurfaces in large-scale displays.
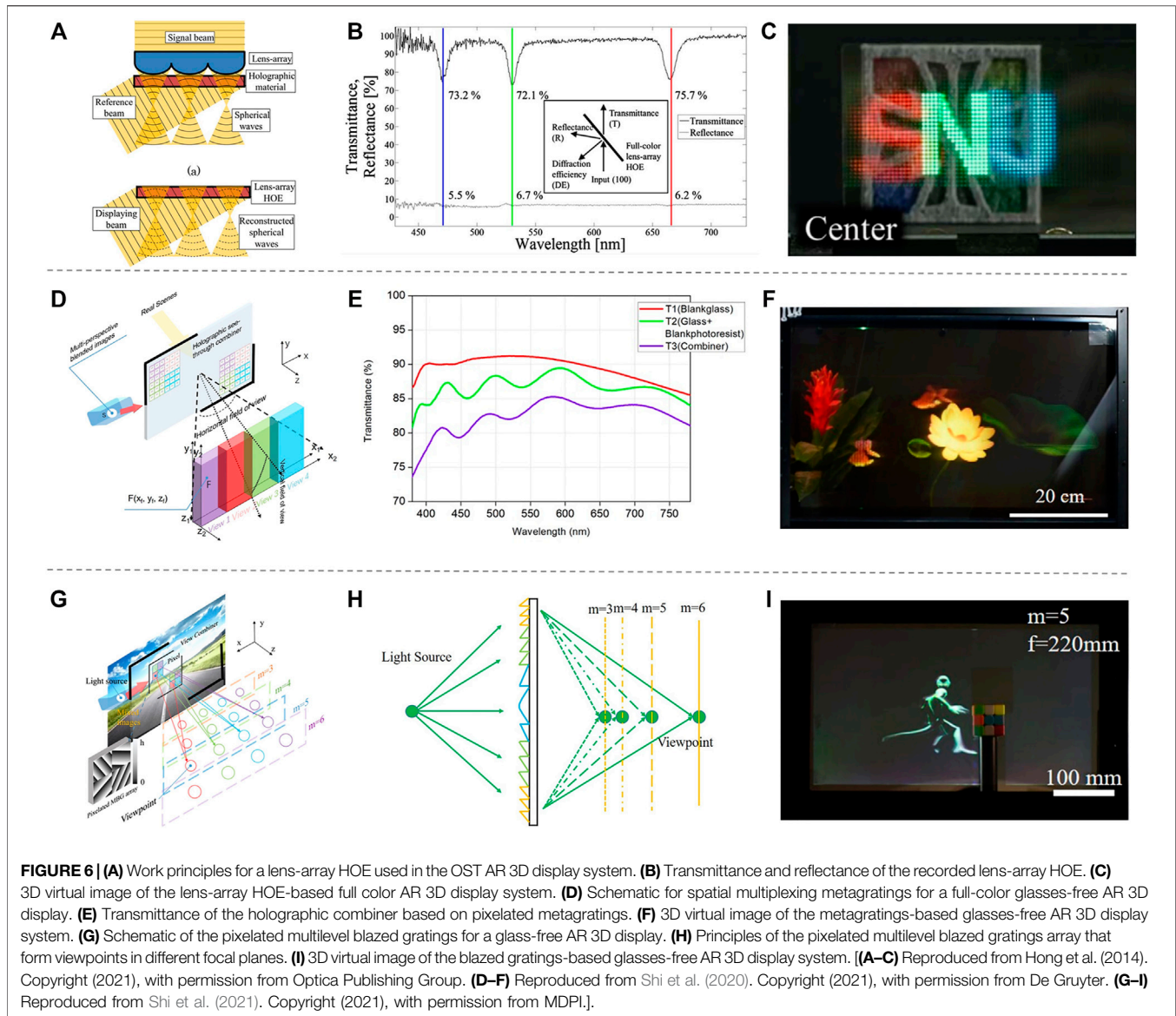
GLASSES-FREE AUGMENTED REALITY 3D DISPLAY BASED ON PLANAR OPTICAL ELEMENTS

Most recently, augmented reality (AR), as an interactive display that fuses the virtual world with reality, has become an aggressive research field that attracts broad attention from researchers, investors and scientists (Chang et al., 2020; Xiong et al., 2021). Glasses-free AR 3D displays are of special interest because of the huge demand in many applications, such as head-up displays in vehicles, education, and exhibitions. Although near-to-eye displays for AR technologies based on wearable devices can be implemented by various methods, including free-form optics, holographic optical elements, surface relief gratings, or metasurfaces, the realization of glasses-free AR 3D displays is a much harder task because of the uncertain spatial relationship between the display screen and observers. Glasses-free AR 3D displays can be assigned to either reflection-type and optical see-through type displays. Li et al. adopted a mirror-based pinhole array to demonstrate a reflective AR 3D display system based on an integral imaging display (Li et al., 2019). Recently, they improved the performance of the reflection-type AR 3D system with high definition and high brightness based on the use of a reflective polarizer (Li et al., 2021). However, in the reflection-type AR 3D display, virtual images are fused with mirror images of the real scene rather than the real scene itself.

The optical see-through glasses-free AR 3D display permits people to perceive real scenes directly through a transparent optical combiner (Hong et al., 2016; Mu et al., 2020). Generally, it occupies the mainstream for various AR 3D display technologies and can be realized by using geometric optical elements, holographic optical elements (HOE) and metagratings. In 2020, a lenticular lens-based light field 3D display system with continuous depth was proposed and integrated into AR head up display optics (Lee et al., 2020). This integrated system can generate stereoscopic virtual images with a FOV of 10° × 5°.

The HOE is an optical component that can be used to produce holographic images using principles of diffraction, which is commonly used in transparent displays, 3D imaging, and certain scanning technologies. HOEs share the same optical functions as conventional optical elements, such as mirrors, microlenses, and lenticular lenses. On the other hand, they also have unique

FIGURE 6 | (A) Work principles for a lens-array HOE used in the OST AR 3D display system. **(B)** Transmittance and reflectance of the recorded lens-array HOE. **(C)** 3D virtual image of the lens-array HOE-based full color AR 3D display system. **(D)** Schematic for spatial multiplexing metagratings for a full-color glasses-free AR 3D display. **(E)** Transmittance of the holographic combiner based on pixelated metagratings. **(F)** 3D virtual image of the metagratings-based glasses-free AR 3D display system. **(G)** Schematic of the pixelated multilevel blazed gratings for a glass-free AR 3D display. **(H)** Principles of the pixelated multilevel blazed gratings array that form viewpoints in different focal planes. **(I)** 3D virtual image of the blazed gratings-based glasses-free AR 3D display system. [**(A–C)** Reproduced from Hong et al. (2014). Copyright (2021), with permission from Optica Publishing Group. **(D–F)** Reproduced from Shi et al. (2020). Copyright (2021), with permission from De Gruyter. **(G–I)** Reproduced from Shi et al. (2021). Copyright (2021), with permission from MDPI.].

advantages of high transparency and high diffraction efficiency. On this basis, the integral imaging display can be integrated with an AR display based on a lenticular lens or microlens-array HOE (Li et al., 2016; Wakunami et al., 2016). Moreover, the HOE can be recorded by wavelength multiplexing for full-color imaging (Hong et al., 2014; Deng et al., 2019) (**Figure 6A**). A high transmittance was achieved at all wavelengths (**Figures 6B,C**). A 2D/3D convertible AR 3D display was further proposed based on a lens-array holographic optical element, a polymer dispersed liquid crystal film, and a projector (Zhang et al., 2019). Controlled by voltage, the film can switch the display mode from a 2D display to an optical see-through 3D display.
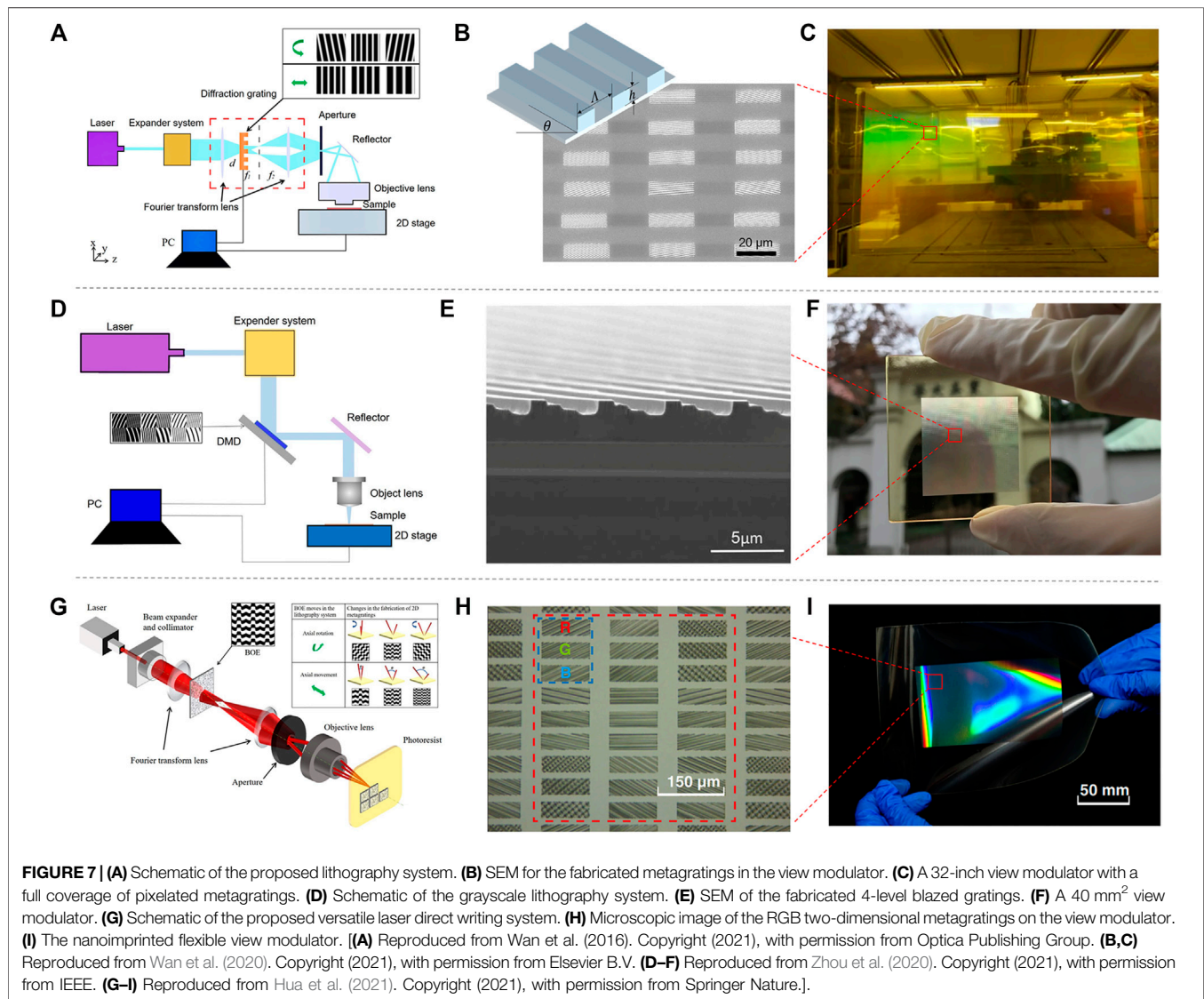
In fact, AR 3D displays based on lens arrays form self-repeating views. Thus, both motion parallax and FOV are limited. Moreover, false depth cues for 3D virtual images can

be generated due to the image flip effect. Correct depth cues are particularly important for AR 3D displays when virtual images fuse with natural objects. On this basis, a holographic combiner composed of spatial multiplexing metagratings was proposed to realize a 32-inch full-color glass-free AR 3D display, as shown in **Figure 6D** (Shi et al., 2020). The irradiance pattern for each view is formed as a super Gaussian function to reduce crosstalk. A FOV as large as 47° was achieved in the horizontal direction. For the sake of correct white balance, three layers of metagratings are stacked for spatial multiplexing. The whole system contains only two components: a projector and a metagrating-based holographic combiner. Moreover, the transmittance is higher than 75% over the visible spectrum (**Figures 6E,F**), but the light efficiency of metagrating is relatively low (40% in theory and 12% in experiment). To improve the light efficiency, pixelated

Glass-free 3D AR displays	Classification	Spatial resolution	FOV	Display size	References
Reflection type	Reflective lens or pinhole array	Low	Small	Large	Li et al. (2019); Li et al. (2021)
Optical see-through type	Geometric optical elements	Low	Small	Large	Lee et al. (2020)
	Lens or Microlens array HOE	Low	Small	Small	Li et al. (2016); Wakunami et al. (2016); Hong et al. (2014); Zhang et al. (2019)
	Lenticular lens array HOE	Middle	Small	Small	Deng et al. (2019)
	Metagrating	Middle	Large	Large	Shi et al. (2020); Shi et al. (2021)

FIGURE 7 | (A) Schematic of the proposed lithography system. **(B)** SEM for the fabricated metagratings in the view modulator. **(C)** A 32-inch view modulator with a full coverage of pixelated metagratings. **(D)** Schematic of the grayscale lithography system. **(E)** SEM of the fabricated 4-level blazed gratings. **(F)** A 40 mm² view modulator. **(G)** Schematic of the proposed versatile laser direct writing system. **(H)** Microscopic image of the RGB two-dimensional metagratings on the view modulator. **(I)** The nanoimprinted flexible view modulator. [**(A)** Reproduced from Wan et al. (2016). Copyright (2021), with permission from Optica Publishing Group. **(B,C)** Reproduced from Wan et al. (2020). Copyright (2021), with permission from Elsevier B.V. **(D–F)** Reproduced from Zhou et al. (2020). Copyright (2021), with permission from IEEE. **(G–I)** Reproduced from Hua et al. (2021). Copyright (2021), with permission from Springer Nature.].

multilevel blazed gratings were introduced for glasses-free AR 3D displays with a 20 inch format (**Figures 6G,H**) (Shi et al., 2021). The measured diffraction efficiency was improved to a value of ~53%. The viewing distance for motion parallax was extended to more than 5 m, benefiting from the multiorder

diffraction light according to harmonic diffraction theory (**Figure 6I**).

We introduce a summary of various methods for realizing glasses-free AR 3D displays. As shown in **Table 2**, the optical see-through combiner outweighs the reflection type method

FIGURE 8 | Schematic of the emerging planar optical elements applied in glasses-free 3D displays and glasses-free AR 3D displays. There are various merits for planar optical elements compared with geometric optical elements. DG: Diffraction gratings.
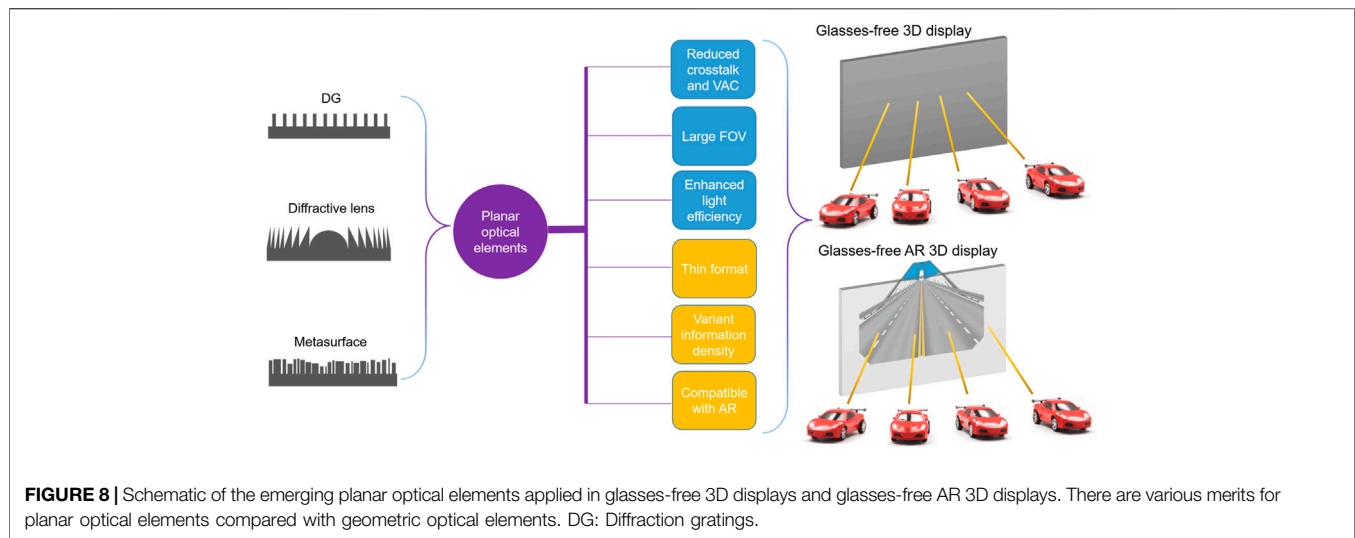
for a more natural fusion with the physical world. In all optical see-through combiners, holographic optical element-based combiners have the advantages of high diffraction efficiency and high transparency. However, they suffer from a limited FOV and motion parallax. The metagrating-based combiner offers an accurate depth cue over a large FOV. The multilevel blazed grating-based method further improves the light efficiency and viewing depth due to multiorder diffraction.

FABRICATION OF LARGE-SCALE MICRO/ NANOSTRUCTURES ON VIEW MODULATORS FOR 3D DISPLAYS

The development of high-throughput micro/nanofabrication methods is essential for large view modulators. To fabricate the diffraction gratings or metagratings at a high throughput, a flexible lithography system was proposed (**Figure 7A**) (Wan et al., 2016). The nanogratings in this system were fabricated pixel by pixel. Through one exposure, a nanograting pixel with a size on the scale of tens of microns was formed. Therefore, the throughput can be much faster than that obtained by an electron beam lithography system that works via a sequential writing process. In addition, the periodic tuning accuracy of the fabricated gratings can be less than 1 nm. Using the proposed lithography system, a 32-inch view modulator with a minimum feature size of 300 nm was successfully prepared for a glass-free 3D display (**Figures 7B,C**). This view modulator has a total of 24,883,200 pixelated metagratings.

To efficiently fabricate multilevel microstructures, a grayscale laser direct writing system can be employed, as shown in **Figure 7D**. The system mainly contains a laser, an electronically programmable spatial light modulator device and an objective lens. The spatial light modulator device loads the hologram patterns that are refreshed synchronously with the movement of the 2D sample stage. The

objective lens reduces the pixel size of the spatial light modulator device by 20 times or 50 times. Furthermore, the proposed laser direct writing system has a high throughput of 25 mm^2/min, which supports the fabrication of a large-scale view modulator for display purposes. It took only 30 min to fabricate a 40 mm^2 view modulator fully covered with a four-level blazed diffractive lens (**Figures 7E,F**).

To enable the fabrication of various complex nanostructures, a versatile laser direct writing system was developed (**Figure 7G**). The key component of the laser direct writing system is a phase-modulated system, which consists of two Fourier transform lenses and a predesign binary optical element inserted in between the lenses. Using the proposed interference lithography system, a 9-inch view modulator fully covered with 2D metagratings was successfully fabricated (**Figures 7H,I**). Moreover, the laser direct writing system has a high processing efficiency of 20 mm^2/min and a high periodic tuning accuracy of 1 nm. Therefore, it shows great potential for the fabrication of metasurfaces.

CONCLUSIONS AND OUTLOOK

In this paper, we mainly focused on the exciting achievements of planar optics-based glass-free 3D displays and glass-free AR 3D displays (as summarized in **Figure 8**). Planar optics opens up the possibility to manipulate the beam steering pixel by pixel, rather than an image with many pixels as in a microlens array-based architecture. There are several benefits to modulating individual pixels. First, the views can be arranged freely either in a line for horizontal parallax, a curve for table-top 3D displays, or a matrix for full parallax. As a result, the views can be arranged according to the application. Second, when imaging with many pixels, many pixels are wasted, especially at large viewing angles. Therefore, severe resolution degradation is always criticized. In the pixel-to-pixel steering strategy, however, every pixel contributes to the virtual 3D image. Third, planar optics offers superior light

steering capability for a large FOV. Fourth, the light distribution of each view can be tuned from a Gaussian distribution to a super-Gaussian distribution to minimize crosstalk and ghost images. Fifth, the view shape can be tuned to dots/linear/rectangular shapes for information density variant 3D displays. The tradeoff between resolution and viewing angle can be alleviated. Sixth, a super multiview display can be realized with closely packaged views to address vergence-accommodation conflict problems. Seventh, multilevel structures, such as blazed gratings, diffractive lenses, and metasurfaces, offer solutions for high light efficiency and reduced chromatic aberration. Eighth, planar optics possess the features of a thin form factor and light weight, which are compatible with portable electronics. Finally, a glass-free AR 3D display can be achieved with a large FOV, enhanced light efficiency and reduced crosstalk for window displays.

To summarize, planar optics-based 3D displays have the advantages of a thin form factor, light weight, flexible design, and precise light manipulation. They hold great promise to tackle the critical challenges for geometric-based 3D displays, especially for the applications of portable electronics and transparent displays.

Future research in planar optics-based 3D displays should focus on the improvement of display performance and enhancement of practicality. From the system level, some strategies can be used to further improve display performance. First, a time-multiplexed strategy enabled by a high refresh rate monitor can be used to increase the resolution by exploiting the redundant time information (Hwang et al., 2014; Ting et al., 2016; Liu et al., 2019). For example, a projector array and a liquid crystal-based steering screen has been used to implement a time-multiplexed multiview 3D display. An angular steering screen was used to control the light direction to generate more continual viewpoints, thereby increasing the angular resolution (Xia et al., 2018). In another work, a time sequential directional beam splitter array was introduced in a multiview 3D display to increase the spatial resolution (Feng et al., 2017). When equipped with eye-tracking systems, a time-multiplexed 3D display can provide both high spatial resolution and angular resolution for single-user applications. Second, a foveated vision strategy can be utilized to compress the image processing load and improve the optical performance of the imaging system and near-eye display (Phillips et al., 2017; Chang et al., 2020). For instance, a multiresolution foveated display using two display panels and an optical combiner was proposed for virtual reality applications (Tan et al., 2018). The first display panel provides a wide FOV, and the second display panel improves spatial resolution for the central fovea region. This system effectively reduces the screen-door effect in near-eye displays. Moreover, a foveated glasses-free 3D display was also demonstrated with spatially variant information density. This strategy offers potential solutions to solve the trade-off between resolution and FOV (Hua et al., 2021). For foveated display systems, liquid crystal lens technology is also significant (Chen et al., 2015; Lin et al., 2017; Yuan et al., 2021).

Under polarization control, liquid crystal lenses with tunable focal lengths are able to provide active switching of the FOV. This technology was demonstrated in a foveated near-eye display to create multiresolution images with a single display module (Yoo et al., 2020). The system maintains both a wide FOV and high resolution with compressed data. Third, the development of artificial intelligence algorithms can improve the optical performance of planar optical elements (Chang et al., 2018; Sitzmann et al., 2018; Tseng et al., 2021; Zeng et al., 2021). For example, an end-to-end optimization algorithm was introduced to design a diffractive achromatic lens. By jointly learning the lens and an image recovery neural network, this method can be used to realize superior high-fidelity imaging (Dun et al., 2020). Therefore, in planar optics-based 3D displays, algorithms such as deep learning can be incorporated with hardware for aberration reduction and image precalibration.

In addition to the aforementioned improvement in display performance, several techniques need to be implemented that can promote the practical application of 3D displays. First, a directional backlight system with low divergence and high uniformity should be integrated into planar optics-based glass-free 3D displays (Yoon et al., 2011; Fan et al., 2015; Teng and Tseng, 2015; Zhan et al., 2016; Krebs et al., 2017). The angular divergence of the illumination greatly affects the display performance in terms of crosstalk and ghost images. An edge-lit directional backlight based on a waveguide with pixelated nanogratings was proposed (Zhang et al., 2020). The directional backlight module provides an angular divergence of ±6.17° and a uniformity of 95.7 and 86.8% in the x- and y-directions, respectively, at a wavelength of 532 nm. In another work, a steering-backlight was introduced into a slim panel holographic video display (An et al., 2020). The overall system thickness is < 10 cm. Nevertheless, the design and fabrication of a directional backlight is still a difficult task. Second, several challenges in nanofabrication should be overcome for planar optics-based 3D displays (Manfrinato et al., 2013; Manfrinato et al., 2014; Chen et al., 2015; Qiao et al., 2016; Wu et al., 2021). For example, the patterning of nanostructures over a large size, the fabrication of multilevel micro/nanostructures with a high aspect ratio, and the realization of high-fidelity batch copies of micro/nanostructures remains challenging. We believe that numerous micro/nanomanufacturing techniques and instruments will be developed to meet the specific needs of 3D displays. Last but not least, planar optics-based 3D displays will benefit from the rapid development of advanced display panels. To enhance the brightness while ensuring low system power consumption, a spontaneous emission source can be introduced into planar optics-based 3D displays (Fang et al., 2006; Hoang et al., 2015; Pelton, 2015). By constructing plasmonic nanoantennas, large spontaneous emission enhancements were realized with increased spontaneous emission rates (Tsakmakidis et al., 2016). As a result, light-emitting diodes can possess a faster modulation speed than typical semiconductor lasers, providing a solution with high brightness and a high refresh rate. Ideally, the space-bandwidth product needs to be larger than 50 K for glasses-free 3D displays. MicroLED and nanoLED displays can effectively expand space-bandwidth products and fundamentally solve the problem of resolution degradation in the future (Huang et al., 2020; Liu

et al., 2020). We believe that advances in directional backlights, nanofabrication, spontaneous emission sources, and microLED displays will lead to innovative and ecological development of the 3D display industry.

AUTHOR CONTRIBUTIONS

JH drafted the manuscript. WQ and LC revised and provided their valuable inputs to further improve the manuscript. All authors contributed to the article and approved the submitted version.

REFERENCES

An, J., Won, K., Kim, Y., Hong, J.-Y., Kim, H., Kim, Y., et al. (2020). Slim-panel Holographic Video Display. *Nat. Commun.* 11 (1), 1–7. doi:10.1038/s41467-020-19298-4

Banerji, S., Meem, M., Majumder, A., Sensale-Rodriguez, B., and Menon, R. (2020). Extreme-depth-of-focus Imaging with a Flat Lens. *Optica* 7 (3), 214–217. doi:10.1364/OPTICA.384164

Banerji, S., Meem, M., Majumder, A., Vasquez, F. G., Sensale-Rodriguez, B., and Menon, R. (2019). Imaging with Flat Optics: Metalenses or Diffractive Lenses? *Optica* 6 (6), 805–810. doi:10.1364/OPTICA.6.000805

Banerji, S., and Sensale-Rodriguez, B. (2019). A Computational Design Framework for Efficient, Fabrication Error-Tolerant, Planar THz Diffractive Optical Elements. *Sci. Rep.* 9 (1), 1–9. doi:10.1038/s41598-019-42243-5

Blanche, P.-A., Bablumian, A., Voorakaranam, R., Christenson, C., Lin, W., Gu, T., et al. (2010). Holographic Three-Dimensional Telepresence Using Large-Area Photorefractive Polymer. *Nature* 468 (7320), 80–83. doi:10.1038/nature09521

Cao, Y., Wang, P. X., D'Acierno, F., Hamad, W. Y., Michal, C. A., and MacLachlan, M. J. (2020). Tunable Diffraction Gratings from Biosourced Lyotropic Liquid Crystals. *Adv. Mater.* 32 (19), 1907376. doi:10.1002/adma.201907376

Chang, C., Bang, K., Wetzstein, G., Lee, B., and Gao, L. (2020). Toward the Next-Generation VR/AR Optics: a Review of Holographic Near-Eye Displays from a Human-Centric Perspective. *Optica* 7 (11), 1563–1578. doi:10.1364/OPTICA.406004

Chang, C., Cui, W., and Gao, L. (2020). Foveated Holographic Near-Eye 3D Display. *Opt. Express* 28 (2), 1345–1356. doi:10.1364/OE.384421

Chang, J., Sitzmann, V., Dun, X., Heidrich, W., and Wetzstein, G. (2018). Hybrid Optical-Electronic Convolutional Neural Networks with Optimized Diffractive Optics for Image Classification. *Sci. Rep.* 8 (1), 1–10. doi:10.1038/s41598-018-30619-y

Charles, W. (1838). XVIII. Contributions to the Physiology of Vision. -Part the First. On Some Remarkable, and Hitherto Unobserved, Phenomena of Binocular Vision. *Phil. Trans. R. Soc.* 128, 371–394. doi:10.1098/rstl.1838.0019

Chen, W. T., Zhu, A. Y., Sanjeev, V., Khorasaninejad, M., Shi, Z., Lee, E., et al. (2018). A Broadband Achromatic Metalens for Focusing and Imaging in the Visible. *Nat. Nanotech* 13 (3), 220–226. doi:10.1038/s41565-017-0034-6

Chen, Y. (2015). Nanofabrication by Electron Beam Lithography and its Applications: A Review. *Microelectronic Eng.* 135, 57–72. doi:10.1016/j.mee.2015.02.042

Chen, Z., and Segev, M. (2021). Highlighting Photonics: Looking into the Next Decade. *eLight* 1 (1), 1–12. doi:10.1186/s43593-021-00002-y

Deng, H., Chen, C., He, M.-Y., Li, J.-J., Zhang, H.-L., and Wang, Q.-H. (2019). High-resolution Augmented Reality 3D Display with Use of a Lenticular Lens Array Holographic Optical Element. *J. Opt. Soc. Am. A.* 36 (4), 588–593. doi:10.1364/JOSAA.36.000588

Dodgson, N. A. (2005). Autostereoscopic 3D Displays. *Computer* 38 (8), 31–36. doi:10.1109/MC.2005.252

Dun, X., Ikoma, H., Wetzstein, G., Wang, Z., Cheng, X., and Peng, Y. (2020). Learned Rotationally Symmetric Diffractive Achromat for Full-Spectrum Computational Imaging. *Optica* 7 (8), 913–922. doi:10.1364/OPTICA.394413

Ergin, T., Stenger, N., Brenner, P., Pendry, J. B., and Wegener, M. (2010). Three-dimensional Invisibility Cloak at Optical Wavelengths. *Science* 328 (5976), 337–339. doi:10.1126/science.1186351

Faklis, D., and Morris, G. M. (1995). Spectral Properties of Multiorder Diffractive Lenses. *Appl. Opt.* 34 (14), 2462–2468. doi:10.1364/AO.34.002462

Fan, H., Zhou, Y., Wang, J., Liang, H., Krebs, P., Su, J., et al. (2015). Full Resolution, Low Crosstalk, and Wide Viewing Angle Auto-Stereoscopic Display with a Hybrid Spatial-Temporal Control Using Free-form Surface Backlight Unit. *J. Display Technol.* 11 (7), 620–624. doi:10.1109/JDT.2015.2425432

Fan, Z.-B., Qiu, H.-Y., Zhang, H.-L., Pang, X.-N., Zhou, L.-D., Liu, L., et al. (2019). A Broadband Achromatic Metalens Array for Integral Imaging in the Visible. *Light Sci. Appl.* 8 (1), 1–10. doi:10.1038/s41377-019-0178-2

Fang, A. W., Park, H., Cohen, O., Jones, R., Paniccia, M. J., and Bowers, J. E. (2006). Electrically Pumped Hybrid AlGaInAs-Silicon Evanescent Laser. *Opt. Express* 14 (20), 9203–9210. doi:10.1364/OE.14.009203

Faraji-Dana, M., Arbabi, E., Arbabi, A., Kamali, S. M., Kwon, H., and Faraon, A. (2018). Compact Folded Metasurface Spectrometer. *Nat. Commun.* 9 (1), 1–8. doi:10.1038/s41467-018-06495-5

Fattal, D., Peng, Z., Tran, T., Vo, S., Fiorentino, M., Brug, J., et al. (2013). A Multi-Directional Backlight for a Wide-Angle, Glasses-free Three-Dimensional Display. *Nature* 495 (7441), 348–351. doi:10.1038/nature11972

Feng, J.-L., Wang, Y.-J., Liu, S.-Y., Hu, D.-C., and Lu, J.-G. (2017). Three-dimensional Display with Directional Beam Splitter Array. *Opt. Express* 25 (2), 1564. doi:10.1364/OE.25.001564

Fleming, M. B., and Hutley, M. C. (1997). Blazed Diffractive Optics. *Appl. Opt.* 36 (20), 4635–4643. doi:10.1364/AO.36.004635

Genevet, P., Capasso, F., Aieta, F., Khorasaninejad, M., and Devlin, R. (2017). Recent Advances in Planar Optics: from Plasmonic to Dielectric Metasurfaces. *Optica* 4 (1), 139–152. doi:10.1364/OPTICA.4.000139

Geng, J. (2013). Three-dimensional Display Technologies. *Adv. Opt. Photon.* 5 (4), 456–535. doi:10.1364/AOP.5.000456

Görrn, P., Lehnhardt, M., Kowalsky, W., Riedl, T., and Wagner, S. (2011). Elastically Tunable Self-Organized Organic Lasers. *Adv. Mater.* 23 (7), 869–872. doi:10.1002/adma.201003108

Hahn, J., Kim, H., Lim, Y., Park, G., and Lee, B. (2008). Wide Viewing Angle Dynamic Holographic Stereogram with a Curved Array of Spatial Light Modulators. *Opt. Express* 16 (16), 12372–12386. doi:10.1364/OE.16.012372

Heide, F., Fu, Q., Peng, Y., and Heidrich, W. (2016). Encoded Diffractive Optics for Full-Spectrum Computational Imaging. *Sci. Rep.* 6 (1), 1–10. doi:10.1038/srep33543

Hirayama, R., Martinez Plasencia, D., Masuda, N., and Subramanian, S. (2019). A Volumetric Display for Visual, Tactile and Audio Presentation Using Acoustic Trapping. *Nature* 575 (7782), 320–323. doi:10.1038/s41586-019-1739-5

Hoang, T. B., Akselrod, G. M., Argyropoulos, C., Huang, J., Smith, D. R., and Mikkelsen, M. H. (2015). Ultrafast Spontaneous Emission Source Using Plasmonic Nanoantennas. *Nat. Commun.* 6 (1), 1–7. doi:10.1038/ncomms8788

Hong, J.-Y., Park, S.-G., Lee, C.-K., Moon, S., Kim, S.-J., Hong, J., et al. (2016). See-through Multi-Projection Three-Dimensional Display Using Transparent Anisotropic Diffuser. *Opt. Express* 24 (13), 14138–14151. doi:10.1364/OE.24.014138

Hong, K., Yeom, J., Jang, C., Hong, J., and Lee, B. (2014). Full-color Lens-Array Holographic Optical Element for Three-Dimensional Optical See-Through Augmented Reality. *Opt. Lett.* 39 (1), 127–130. doi:10.1364/OL.39.000127

Hua, J., Hua, E., Zhou, F., Shi, J., Wang, C., Duan, H., et al. (2021). Foveated Glasses-free 3D Display with Ultrawide Field of View via a Large-Scale 2D-Metagrating Complex. *Light Sci. Appl.* 10 (1), 1–9. doi:10.1038/s41377-021-00651-1

Hua, J., Yi, D., Qiao, W., and Chen, L. (2020). Multiview Holographic 3D Display Based on Blazed Fresnel DOE. *Opt. Commun.* 472, 125829. doi:10.1016/j.optcom.2020.125829

Huang, F., Liu, H., Ye, H., Qiu, C.-W., Hong, M., et al. (2018). Planar Diffractive Lenses: Fundamentals, Functionalities, and Applications. *Adv. Mater.* 30 (26), 1704556. doi:10.1002/adma.201704556

Huang, L., Chen, X., Mühlenbernd, H., Zhang, H., Chen, S., Bai, B., et al. (2013). Three-dimensional Optical Holography Using a Plasmonic Metasurface. *Nat. Commun.* 4 (1), 1–8. doi:10.1038/ncomms3808

Huang, L., Zhang, S., and Zentgraf, T. (2018). Metasurface Holography: from Fundamentals to Applications. *Nanophotonics* 7 (6), 1169–1190. doi:10.1515/nanoph-2017-0118

Huang, T., Han, B., Zhang, X., and Liao, H. (2019). High-performance Autostereoscopic Display Based on the Lenticular Tracking Method. *Opt. Express* 27 (15), 20421–20434. doi:10.1364/OE.27.020421

Huang, Y., Hsiang, E.-L., Deng, M.-Y., and Wu, S.-T. (2020). Mini-LED, Micro-LED and OLED Displays: Present Status and Future Perspectives. *Light Sci. Appl.* 9 (1), 1–16. doi:10.1038/s41377-020-0341-9

Hwang, Y. S., Bruder, F.-K., Fäcke, T., Kim, S.-C., Walze, G., Hagen, R., et al. (2014). Time-sequential Autostereoscopic 3-D Display with a Novel Directional Backlight System Based on Volume-Holographic Optical Elements. *Opt. Express* 22 (8), 9820–9838. doi:10.1364/OE.22.009820

Intaravanne, Y., Han, J., Wang, R., Ma, A., Li, S., Chen, S., et al. (2021). Phase Manipulation-Based Polarization Profile Realization and Hybrid Holograms Using Geometric Metasurface. *Adv. Photo. Res.* 2 (7), 2000046. doi:10.1002/adpr.202000046

Ives, F. E. (1902). A Novel Stereogram. *J. Franklin Inst.* 153 (1), 51–52. doi:10.1016/S0016-0032(02)90195-X

Javidi, B., Carnicer, A., Arai, J., Fujii, T., Hua, H., Liao, H., et al. (2020). Roadmap on 3D Integral Imaging: Sensing, Processing, and Display. *Opt. Express* 28 (22), 32266–32293. doi:10.1364/OE.402193

Jiang, Q., Jin, G., and Cao, L. (2019). When Metasurface Meets Hologram: Principle and Advances. *Adv. Opt. Photon.* 11 (3), 518–576. doi:10.1364/AOP.11.000518

Khorasaninejad, M., Chen, W. T., Devlin, R. C., Oh, J., Zhu, A. Y., and Capasso, F. (2016). Metalenses at Visible Wavelengths: Diffraction-Limited Focusing and Subwavelength Resolution Imaging. *Science* 352 (6290), 1190–1194. doi:10.1126/science.aaf6644

Kim, S.-U., Kim, J., Suh, J.-H., Na, J.-H., and Lee, S.-D. (2016). Concept of Active Parallax Barrier on Polarizing Interlayer for Near-Viewing Autostereoscopic Displays. *Opt. Express* 24 (22), 25010–25018. doi:10.1364/OE.24.025010

Koulieris, G.-A., Bui, B., Banks, M. S., and Drettakis, G. (2017). Accommodation and comfort in Head-Mounted Displays. *ACM Trans. Graph.* 36 (4), 1–11. doi:10.1145/3072959.3073622

Krebs, P., Liang, H., Fan, H., Zhang, A., Zhou, Y., Chen, J., et al. (2017). Homogeneous Free-form Directional Backlight for 3D Display. *Opt. Commun.* 397, 112–117. doi:10.1016/j.optcom.2017.04.002

Kumagai, K., Suzuki, D., Hasegawa, S., and Hayasaki, Y. (2015). Volumetric Display with Holographic Parallel Optical Access and Multilayer Fluorescent Screen. *Opt. Lett.* 40 (14), 3356–3359. doi:10.1364/OL.40.003356

Kumagai, K., Yamaguchi, I., and Hayasaki, Y. (2018). Three-dimensionally Structured Voxels for Volumetric Display. *Opt. Lett.* 43 (14), 3341–3344. doi:10.1364/OL.43.003341

Lanman, D., Hirsch, M., Kim, Y., and Raskar, R. (2010). Content-adaptive Parallax Barriers. *ACM Trans. Graph.* 29 (6), 1–10. doi:10.1145/1866158.186616410.1145/1882261.1866164

Lanman, D., Wetzstein, G., Hirsch, M., Heidrich, W., and Raskar, R. (2011). Polarization fields. *ACM Trans. Graph.* 30 (6), 1–10. doi:10.1145/2024156.202422010.1145/2070781.2024220

Lee, B., Kim, D., Lee, S., Chen, C., and Lee, B. (2022). *High-contrast, Speckle-free, True 3D Holography via Binary CGH Optimization.* arXiv preprint arXiv:2201.02619.

Lee, J.-h., Yanusik, I., Choi, Y., Kang, B., Hwang, C., Park, J., et al. (2020). Automotive Augmented Reality 3D Head-Up Display Based on Light-Field Rendering with Eye-Tracking. *Opt. Express* 28 (20), 29788–29804. doi:10.1364/OE.404318

Li, G., Lee, D., Jeong, Y., Cho, J., and Lee, B. (2016). Holographic Display for See-Through Augmented Reality Using Mirror-Lens Holographic Optical Element. *Opt. Lett.* 41 (11), 2486–2489. doi:10.1364/OL.41.002486

Li, Q., Deng, H., Pang, S., Jiang, W., and Wang, Q. (2019). A Reflective Augmented Reality Integral Imaging 3D Display by Using a Mirror-Based Pinhole Array. *Appl. Sci.* 9 (15), 3124. doi:10.3390/app9153124

Li, Q., He, W., Deng, H., Zhong, F.-Y., and Chen, Y. (2021). High-performance Reflection-type Augmented Reality 3D Display Using a Reflective Polarizer. *Opt. Express* 29 (6), 9446–9453. doi:10.1364/OE.421879

Liang, H., An, S., Wang, J., Zhou, Y., Fan, H., Krebs, P., et al. (2014). Optimizing Time-Multiplexing Auto-Stereoscopic Displays with a Genetic Algorithm. *J. Display Technol.* 10 (8), 695–699. doi:10.1109/JDT.2014.2314138

Lin, Y.-H., Wang, Y.-J., and Reshetnyak, V. (2017). Liquid crystal Lenses with Tunable Focal Length. *Liquid Crystals Rev.* 5 (2), 111–143. doi:10.1080/21680396.2018.1440256

Lippmann, G. (1908). Épreuves réversibles donnant la sensation du relief. *J. Phys. Theor. Appl.* 7 (1), 821–825. doi:10.1051/jphystap:019080070082100

Liu, B., Sang, X., Yu, X., Gao, X., Liu, L., Gao, C., et al. (2019). Time-multiplexed Light Field Display with 120-degree Wide Viewing Angle. *Opt. Express* 27 (24), 35728–35739. doi:10.1364/OE.27.035728

Liu, Z., Cui, Q., Huang, Z., and Guo, L. J. (2020). Transparent Colored Display Enabled by Flat Glass Waveguide and Nanoimprinted Multilayer Gratings. *ACS Photon.* 7 (6), 1418–1424. doi:10.1021/acsphotonics.9b01803

Liu, Z., Lin, C.-H., Hyun, B.-R., Sher, C.-W., Lv, Z., Luo, B., et al. (2020). Micro-light-emitting Diodes with Quantum Dots in Display Technology. *Light Sci. Appl.* 9 (1), 1–23. doi:10.1038/s41377-020-0268-1

Lv, G.-J., Wang, Q.-H., Zhao, W.-X., Wang, J., Deng, H., and Wu, F. (2015). Glasses-free Three-Dimensional Display Based on Microsphere-Lens Array. *J. Display Technol.* 11 (3), 292–295. doi:10.1109/JDT.2014.2385098

Lv, G.-J., Zhao, B.-C., Wu, F., Zhao, W.-X., Yang, Y.-Z., and Wang, Q.-H. (2017). Autostereoscopic 3D Display with High Brightness and Low Crosstalk. *Appl. Opt.* 56 (10), 2792–2795. doi:10.1364/AO.56.002792

Ma, Q., Cao, L., He, Z., and Zhang, S. (2019). Progress of Three-Dimensional Light-Field Display [Invited]. 中国光学快报 17 (11), 111001. doi:10.3788/COL201917.111001

Maimone, A., Wetzstein, G., Hirsch, M., Lanman, D., Raskar, R., and Fuchs, H. (2013). Focus 3D. *ACM Trans. Graph.* 32 (5), 1–13. doi:10.1145/2503144

Manfrinato, V. R., Wen, J., Zhang, L., Yang, Y., Hobbs, R. G., Baker, B., et al. (2014). Determining the Resolution Limits of Electron-Beam Lithography: Direct Measurement of the point-spread Function. *Nano Lett.* 14 (8), 4406–4412. doi:10.1021/nl5013773

Manfrinato, V. R., Zhang, L., Su, D., Duan, H., Hobbs, R. G., Stach, E. A., et al. (2013). Resolution Limits of Electron-Beam Lithography toward the Atomic Scale. *Nano Lett.* 13 (4), 1555–1558. doi:10.1021/nl304715p

Martínez-Corral, M., and Javidi, B. (2018). Fundamentals of 3D Imaging and Displays: a Tutorial on Integral Imaging, Light-Field, and Plenoptic Systems. *Adv. Opt. Photon.* 10 (3), 512–566. doi:10.1364/AOP.10.000512

Meem, M., Banerji, S., Majumder, A., Vasquez, F. G., Sensale-Rodriguez, B., and Menon, R. (2019). Broadband Lightweight Flat Lenses for Long-Wave Infrared Imaging. *Proc. Natl. Acad. Sci. U.S.A.* 116 (43), 21375–21378. doi:10.1073/pnas.1908447116

Meem, M., Majumder, A., and Menon, R. (2018). Full-color Video and Still Imaging Using Two Flat Lenses. *Opt. Express* 26 (21), 26866–26871. doi:10.1364/OE.26.026866

MIT Technology Review (2013). *Mike Orcutt*. Available at: https://www.technologyreview.com/innovator/david-fattal (Accessed August 21, 2013).

Mohammad, N., Meem, M., Shen, B., Wang, P., and Menon, R. (2018). Broadband Imaging with One Planar Diffractive Lens. *Sci. Rep.* 8 (1), 1–6. doi:10.1038/s41598-018-21169-4

Mohammad, N., Meem, M., Wan, X., and Menon, R. (2017). Full-color, Large Area, Transmissive Holograms Enabled by Multi-Level Diffractive Optics. *Sci. Rep.* 7 (1), 1–6. doi:10.1038/s41598-017-06229-5

Mu, C.-T., Tseng, S.-H., and Chen, C.-H. (2020). See-through Holographic Display with Randomly Distributed Partial Computer Generated Holograms. *Opt. Express* 28 (24), 35674–35681. doi:10.1364/OE.405203

Pelton, M. (2015). Modified Spontaneous Emission in Nanophotonic Structures. *Nat. Photon* 9 (7), 427–435. doi:10.1038/NPHOTON.2015.103

Peng, Y., Choi, S., Kim, J., and Wetzstein, G. (2021). Speckle-free Holography with Partially Coherent Light Sources and Camera-In-The-Loop Calibration. *Sci. Adv.* 7 (46), eabg5040. doi:10.1126/sciadv.abg5040

Peng, Y., Fu, Q., Amata, H., Su, S., Heide, F., and Heidrich, W. (2015). Computational Imaging Using Lightweight Diffractive-Refractive Optics. *Opt. Express* 23 (24), 31393–31407. doi:10.1364/OE.23.031393

Peng, Y., Fu, Q., Heide, F., and Heidrich, W. (2016). The Diffractive Achromat Full Spectrum Computational Imaging with Diffractive Optics. *ACM Trans. Graph.* 35 (4), 1–11. doi:10.1145/2897824.2925941

Peng, Y., Sun, Q., Dun, X., Wetzstein, G., Heidrich, W., and Heide, F. (2019). Learned Large Field-Of-View Imaging with Thin-Plate Optics. *ACM Trans. Graph.* 38 (6), 1–14. doi:10.1145/3355089.3356526

Phillips, D. B., Sun, M.-J., Taylor, J. M., Edgar, M. P., Barnett, S. M., Gibson, G. M., et al. (2017). Adaptive Foveated Single-Pixel Imaging with Dynamic Supersampling. *Sci. Adv.* 3 (4), e1601782. doi:10.1126/sciadv.1601782

Qian, Q., Sun, T., Yan, Y., and Wang, C. (2017). Large-Area Wide-Incident-Angle Metasurface Perfect Absorber in Total Visible Band Based on Coupled Mie Resonances. *Adv. Opt. Mater.* 5 (13), 1700064. doi:10.1002/adom.201700064

Qiao, W., Huang, W., Liu, Y., Li, X., Chen, L.-S., and Tang, J.-X. (2016). Toward Scalable Flexible Nanomanufacturing for Photonic Structures and Devices. *Adv. Mater.* 28 (47), 10353–10380. doi:10.1002/adma.201601801

Sasaki, H., Yamamoto, K., Wakunami, K., Ichihashi, Y., Oi, R., and Senoh, T. (2014). Large Size Three-Dimensional Video by Electronic Holography Using Multiple Spatial Light Modulators. *Sci. Rep.* 4 (1), 1–8. doi:10.1038/srep06177

Shelby, R. A., Smith, D. R., and Schultz, S. (2001). Experimental Verification of a Negative index of Refraction. *Science* 292 (5514), 77–79. doi:10.1126/science.1058847

Shi, J., Hua, J., Zhou, F., Yang, M., and Qiao, W. (2021). Augmented Reality Vector Light Field Display with Large Viewing Distance Based on Pixelated Multilevel Blazed Gratings. *Photonics* 8 (8), 337. doi:10.3390/photonics8080337

Shi, J., Qiao, W., Hua, J., Li, R., and Chen, L. (2020). Spatial Multiplexing Holographic Combiner for Glasses-free Augmented Reality. *Nanophotonics* 9 (9), 3003–3010. doi:10.1515/nanoph-2020-0243

Shi, L., Li, B., Kim, C., Kellnhofer, P., and Matusik, W. (2021). Towards Real-Time Photorealistic 3D Holography with Deep Neural Networks. *Nature* 591 (7849), 234–239. doi:10.1038/s41586-020-03152-0

Sitzmann, V., Diamond, S., Peng, Y., Dun, X., Boyd, S., Heidrich, W., et al. (2018). End-to-end Optimization of Optics and Image Processing for Achromatic Extended Depth of Field and Super-resolution Imaging. *ACM Trans. Graph.* 37 (4), 1–13. doi:10.1145/3197517.3201333

Smalley, D. E., Nygaard, E., Squire, K., Van Wagoner, J., Rasmussen, J., Gneiting, S., et al. (2018). A Photophoretic-Trap Volumetric Display. *Nature* 553 (7689), 486–490. doi:10.1038/nature25176

Sweeney, D. W., and Sommargren, G. E. (1995). Harmonic Diffractive Lenses. *Appl. Opt.* 34 (14), 2469–2475. doi:10.1364/AO.34.002469

Tabiryan, N. V., Roberts, D. E., Liao, Z., Hwang, J. Y., Moran, M., Ouskova, O., et al. (2021). Advances in Transparent Planar Optics: Enabling Large Aperture, Ultrathin Lenses. *Adv. Opt. Mater.* 9 (5), 2001692. doi:10.1002/adom.202001692

Tan, G., Lee, Y.-H., Zhan, T., Yang, J., Liu, S., Zhao, D., et al. (2018). Foveated Imaging for Near-Eye Displays. *Opt. Express* 26 (19), 25076–25085. doi:10.1364/OE.26.025076

Tay, S., Blanche, P.-A., Voorakaranam, R., Tunç, A. V., Lin, W., Rokutanda, S., et al. (2008). An Updatable Holographic Three-Dimensional Display. *Nature* 451 (7179), 694–698. doi:10.1038/nature06596

Teng, T.-C., and Tseng, L.-W. (2015). Design of a Bidirectional Backlight Using a Pair of Stacked Light Guide Plates for Large Dual-View and 3D Displays. *Appl. Opt.* 54 (3), 509–516. doi:10.1364/AO.54.000509

Ting, C.-H., Chang, Y.-C., Chen, C.-H., Huang, Y.-P., and Tsai, H.-W. (2016). Multi-user 3D Film on a Time-Multiplexed Side-Emission Backlight System. *Appl. Opt.* 55 (28), 7922–7928. doi:10.1364/AO.55.007922

Tsakmakidis, K. L., Boyd, R. W., Yablonovitch, E., and Zhang, X. (2016). Large Spontaneous-Emission Enhancements in Metallic Nanostructures: towards LEDs Faster Than Lasers [Invited]. *Opt. Express* 24 (16), 17916–17927. doi:10.1364/OE.24.017916

Tseng, E., Colburn, S., Whitehead, J., Huang, L., Baek, S.-H., Majumdar, A., et al. (2021). Neural Nano-Optics for High-Quality Thin Lens Imaging. *Nat. Commun.* 12 (1), 1–7. doi:10.1038/s41467-021-26443-0

Valentine, J., Zhang, S., Zentgraf, T., Ulin-Avila, E., Genov, D. A., Bartal, G., et al. (2008). Three-dimensional Optical Metamaterial with a Negative Refractive index. *Nature* 455 (7211), 376–379. doi:10.1038/nature07247

Wakunami, K., Hsieh, P.-Y., Oi, R., Senoh, T., Sasaki, H., Ichihashi, Y., et al. (2016). Projection-type See-Through Holographic Three-Dimensional Display. *Nat. Commun.* 7 (1), 1–7. doi:10.1038/ncomms12954

Wan, W., Qiao, W., Huang, W., Zhu, M., Fang, Z., Pu, D., et al. (2016). Efficient Fabrication Method of Nano-Grating for 3D Holographic Display with Full Parallax Views. *Opt. Express* 24 (6), 6203–6212. doi:10.1364/OE.24.006203

Wan, W., Qiao, W., Huang, W., Zhu, M., Ye, Y., Chen, X., et al. (2017). Multiview Holographic 3D Dynamic Display by Combining a Nano-Grating Patterned Phase Plate and LCD. *Opt. Express* 25 (2), 1114–1122. doi:10.1364/OE.25.001114

Wan, W., Qiao, W., Pu, D., and Chen, L. (2020). Super Multi-View Display Based on Pixelated Nanogratings under an Illumination of a point Light Source. *Opt. Lasers Eng.* 134, 106258. doi:10.1016/j.optlaseng.2020.106258

Wan, W., Qiao, W., Pu, D., Li, R., Wang, C., Hu, Y., et al. (2020). Holographic Sampling Display Based on Metagratings. *iScience* 23, 100773. doi:10.1016/j.isci.2019.100773

Wang, P., Mohammad, N., and Menon, R. (2016). Chromatic-aberration-corrected Diffractive Lenses for Ultra-broadband Focusing. *Sci. Rep.* 6 (1), 1–7. doi:10.1038/srep21545

Wang, Q. H., Pan, D. D., Li, D. H., Li, X. F., and Zhao, R. L. (2010). Stereoscopic Image Crosstalk Factor for Auto-Stereoscopic Display Based on Parallax Barrier. *J. Optoelectron. Laser* 21, 1058–1061. doi:10.16136/j.joe.l.2010.07.027

Wang, R., Intaravanne, Y., Li, S., Han, J., Chen, S., Liu, J., et al. (2021). Metalens for Generating a Customized Vectorial Focal Curve. *Nano Lett.* 21 (5), 2081–2087. doi:10.1021/acs.nanolett.0c04775

Watanabe, H., Okaichi, N., Sasaki, H., and Kawakita, M. (2020). Pixel-density and Viewing-Angle Enhanced Integral 3D Display with Parallel Projection of Multiple UHD Elemental Images. *Opt. Express* 28 (17), 24731–24746. doi:10.1364/OE.397647

Wen Qiao, 乔., Fengbin Zhou, 周., and Linsen Chen, 陈. (2020). Towards Application of mobile Devices: the Status and Future of Glasses-free 3D Display. 红外与激光工程 49 (3), 303002. doi:10.3788/IRLA202049.0303002

Wetzstein, G., Lanman, D., Heidrich, W., and Raskar, R. (2011). Layered 3D. *ACM Trans. Graph.* 30 (4), 1–12. doi:10.1145/2010324.1964990

Wetzstein, G., Lanman, D., Hirsch, M., and Raskar, R. (2012). Tensor Displays. *ACM Trans. Graph.* 31 (4), 1–11. doi:10.1145/2185520.2185576

Wu, X., Qiao, W., Zhu, M., Ren, J., Pu, D., and Chen, L. (2021). Roll-to-plate Additive Manufacturing. *Opt. Express* 29 (14), 21833–21843. doi:10.1364/OE.426984

Xia, X., Zhang, X., Zhang, L., Surman, P., and Zheng, Y. (2018). Time-multiplexed Multi-View Three-Dimensional Display with Projector Array and Steering Screen. *Opt. Express* 26 (12), 15528–15538. doi:10.1364/OE.26.015528

Xiong, J., Hsiang, E.-L., He, Z., Zhan, T., and Wu, S.-T. (2021). Augmented Reality and Virtual Reality Displays: Emerging Technologies and Future Perspectives. *Light Sci. Appl.* 10 (1), 1–30. doi:10.1038/s41377-021-00658-8

Xiong, J., and Wu, S.-T. (2021). Planar Liquid crystal Polarization Optics for Augmented Reality and Virtual Reality: From Fundamentals to Applications. *eLight* 1 (1), 1–20. doi:10.1186/s43593-021-00003-x

Yoo, C., Xiong, J., Moon, S., Yoo, D., Lee, C.-K., Wu, S.-T., et al. (2020). Foveated Display System Based on a Doublet Geometric Phase Lens. *Opt. Express* 28 (16), 23690–23702. doi:10.1364/OE.399808

Yoon, H., Oh, S.-G., Kang, D. S., Park, J. M., Choi, S. J., Suh, K. Y., et al. (2011). Arrays of Lucius Microprisms for Directional Allocation of Light and Autostereoscopic Three-Dimensional Displays. *Nat. Commun.* 2 (1), 1–5. doi:10.1038/ncomms1456

Yoon, S. K., Khym, S., Kim, H.-W., and Kim, S.-K. (2016). Variable Parallax Barrier Spacing in Autostereoscopic Displays. *Opt. Commun.* 370, 319–326. doi:10.1016/j.optcom.2016.03.028

Yuan, Z.-N., Cheng, M., Yu, X.-Y., Sun, Z.-B., Li, A.-R., Mukherjee, S., et al. (2021). 33-4: Fast Switchable Multi-Focus Polarization-Dependent Ferroelectric Liquid-Crystal Lenses for Virtual Reality. *SID Symp. Dig. Tech. Pap.* 52 (1), 439–442. doi:10.1002/sdtp.14711

Yue, F., Wen, D., Xin, J., Gerardot, B. D., Li, J., and Chen, X. (2016). Vector Vortex Beam Generation with a Single Plasmonic Metasurface. *ACS Photon.* 3 (9), 1558–1563. doi:10.1021/acsphotonics.6b00392

Zeng, T., Zhu, Y., and Lam, E. Y. (2021). Deep Learning for Digital Holography: a Review. *Opt. Express* 29 (24), 40572–40593. doi:10.1364/OE.443367

Zhan, L., Xu, B., Hu, J., Wang, Y., Li, M., Cao, L., et al. (2016). Directional Backlight 3D Display System with Wide-Dynamic-Range View Zone, High Brightness and Switchable 2D/3D. *J. Display Technol.* 12 (12), 1. doi:10.1109/JDT.2016.2609198

Zhang, H.-L., Deng, H., Li, J.-J., He, M.-Y., Li, D.-H., and Wang, Q.-H. (2019). Integral Imaging-Based 2D/3D Convertible Display System by Using Holographic Optical Element and Polymer Dispersed Liquid crystal. *Opt. Lett.* 44 (2), 387–390. doi:10.1364/OL.44.000387

Zhang, L., Sun, G., Bai, J., Ma, X., Yin, J., Wang, Q., et al. (2020). Realizing Dynamic Diffraction Gratings Based on Light-Direct Writing of Responsive 2D Ordered Patterns. *ACS Mater. Lett.* 2 (9), 1135–1141. doi:10.1021/acsmaterialslett.0c00285

Zhang, Y., and Fang, F. (2019). Development of Planar Diffractive Waveguides in Optical See-Through Head-Mounted Displays. *Precision Eng.* 60, 482–496. doi:10.1016/j.precisioneng.2019.09.009

Zhang, Y., Liu, W., Gao, J., and Yang, X. (2018). Generating Focused 3D Perfect Vortex Beams by Plasmonic Metasurfaces. *Adv. Opt. Mater.* 6 (4), 1701228. doi:10.1002/adom.201701228

Zhang, Y., Yi, D., Qiao, W., and Chen, L. (2020). Directional Backlight Module Based on Pixelated Nano-Gratings. *Opt. Commun.* 459, 125034. doi:10.1016/j.optcom.2019.125034

Zhao, Z.-F., Liu, J., Zhang, Z.-Q., and Xu, L.-F. (2020). Bionic-compound-eye Structure for Realizing a Compact Integral Imaging 3D Display in a Cell Phone with Enhanced Performance. *Opt. Lett.* 45 (6), 1491–1494. doi:10.1364/OL.384182

Zhen Chen, Z., Bo Liu, B., Enhai Liu, E., and Zhangxian Peng, Z. (2016). Adaptive Polarization-Modulated Method for High-Resolution 3D Imaging. *IEEE Photon. Technol. Lett.* 28 (3), 295–298. doi:10.1109/LPT.2015.2495113

Zheng, G., Mühlenbernd, H., Kenney, M., Li, G., Zentgraf, T., and Zhang, S. (2015). Metasurface Holograms Reaching 80% Efficiency. *Nat. Nanotechnol* 10 (4), 308–312. doi:10.1038/NNANO.2015.2

Zhou, F., Hua, J., Shi, J., Qiao, W., and Chen, L. (2020). Pixelated Blazed Gratings for High Brightness Multiview Holographic 3D Display. *IEEE Photon. Technol. Lett.* 32 (5), 283–286. doi:10.1109/LPT.2020.2971147

Zhou, F., Zhou, F., Chen, Y., Hua, J., Qiao, W., and Chen, L. (2022). Vector Light Field Display Based on an Intertwined Flat Lens with Large Depth of Focus. *Optica* 9 (3). doi:10.1364/OPTICA.439613

Zhou, Y., Qin, Z., Liang, Z., Meng, D., Xu, H., Smith, D. R., et al. (2021). Ultra-broadband Metamaterial Absorbers from Long to Very Long Infrared Regime. *Light Sci. Appl.* 10 (1), 1–12. doi:10.1038/s41377-021-00577-8

Zhu, A. Y., Chen, W.-T., Khorasaninejad, M., Oh, J., Zaidi, A., Mishra, I., et al. (2017). Ultra-compact Visible Chiral Spectrometer with Meta-Lenses. *Apl Photon.* 2 (3), 036103. doi:10.1063/1.4974259

Zola, R. S., Bisoyi, H. K., Wang, H., Urbas, A. M., Bunning, T. J., and Li, Q. (2019). Dynamic Control of Light Direction Enabled by Stimuli-Responsive Liquid Crystal Gratings. *Adv. Mater.* 31 (7), 1806172. doi:10.1002/adma.201806172

Zou, B., Liu, Y., Guo, M., and Wang, Y. (2015). EEG-based Assessment of Stereoscopic 3D Visual Fatigue Caused by Vergence-Accommodation Conflict. *J. Display Technol.* 11 (12), 1076–1083. doi:10.1109/JDT.2015.2451087